# An electron microscopy study of wear in polysilicon microelectromechanical systems in ambient air

D.H. Alsem [a,b,c,*], E.A. Stach [d], M.T. Dugger [e], M. Enachescu [b], R.O. Ritchie [a,b]

[a] Department of Materials Science and Engineering, University of California, Berkeley, CA 94720, United States
[b] Materials Sciences Division, Lawrence Berkeley National Laboratory, Berkeley, CA 94720, United States
[c] National Center for Electron Microscopy, Lawrence Berkeley National Laboratory, Berkeley, CA 94720, United States
[d] School of Materials Engineering, Purdue University, West Lafayette, United States
[e] Materials and Process Sciences Center, Sandia National Laboratories, Albuquerque, NM 87185, United States

## Abstract

Wear is a critical factor in determining the durability of microelectromechanical systems (MEMS). While the reliability of polysilicon MEMS has received extensive attention, the mechanisms responsible for this failure mode at the microscale have yet to be conclusively determined. We have used *on-chip* polycrystalline silicon side-wall friction MEMS specimens to study active mechanisms during sliding wear in ambient air. Worn parts were examined by analytical scanning and transmission electron microscopy, while local temperature changes were monitored using advanced infrared microscopy. Observations show that small amorphous debris particles (∼50–100 nm) are removed by fracture through the silicon grains (∼500 nm) and are oxidized during this process. Agglomeration of such debris particles into larger clusters also occurs. Some of these debris particles/clusters create plowing tracks on the beam surface. A nano-crystalline surface layer (∼20–200 nm), with higher oxygen content, forms during wear at and below regions of the worn surface; its formation is likely aided by high local stresses. No evidence of dislocation plasticity or of extreme local temperature increases was found, ruling out the possibility of high temperature-assisted wear mechanisms.
© 2006 Elsevier B.V. All rights reserved.

*Keywords:* Silicon; MEMS; Wear; Electron microscopy

## 1. Introduction

The tribological properties (frictional, lubrication and wear properties) of materials used to fabricate microelectromechanical systems (MEMS) markedly affect their reliability [1–6]. Along with stiction [1,2] and fatigue [7,8], wear is an important failure mechanism in these microsystems. Indeed, the system reliability of MEMS has received an increasing amount of attention [9,10] and there have been some attempts to propose micron-scale wear models for inherently brittle silicon [3–6], which is the main structural material used for MEMS. However, the precise physical processes that cause wear in thin-film silicon have yet to be conclusively determined and are therefore the focus of this paper.

Recent studies on the wear of silicon have shown similar trends in data, yet quite different mechanisms have been proposed to explain the observations. Tanner et al. [3,4] suggested that an adhesive wear mechanism was responsible for failure of silicon microengines. During adhesive wear, asperities on two contacting surfaces adhere, resulting in the asperities cold-welding together. Due to the continuing movement of the surfaces, fracture occurs away from the bonded interface in one of the bodies, leading to augmented asperities and wear debris. Patton et al. [5,6], on the other hand, suggested two separate mechanisms, one for wear in vacuum and one for wear in air. In vacuo, the native oxide layer is presumed to wear off without being regenerated, because of the absence of oxygen and moisture, thereby permitting silicon–silicon bonds to be formed between the two surfaces, which in turn leads to asperity fracture or grain pull-out. Conversely, in air the oxide layer regenerates, causing only silicon dioxide, created by surface reaction of the silicon with oxygen from the air, to continue to wear, without directly wearing the silicon itself. In addition,

---

\* Corresponding author. Department of Materials Science and Engineering, University of California, Berkeley, 1 Cyclotron road MS72-150, Berkeley, CA 94720, United States. Tel.: +1 510 495 2455; fax: +1 510 486 5888.
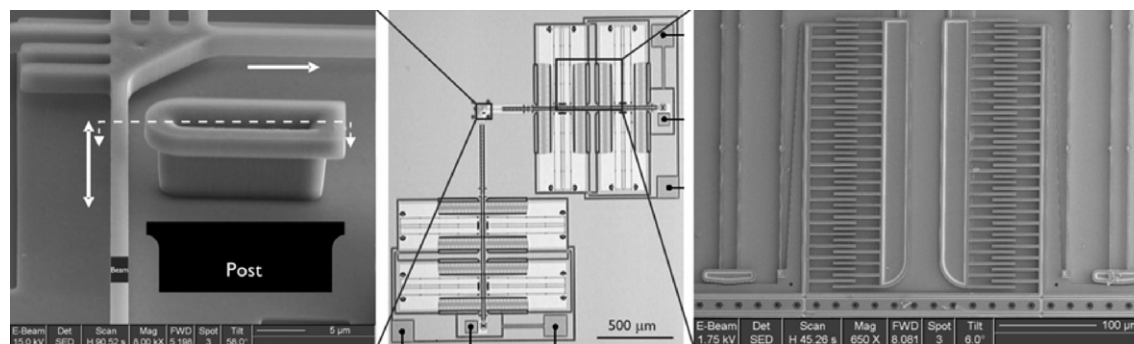*E-mail address:* dhalsem@lbl.gov (D.H. Alsem).

Fig. 1. Polysilicon side-wall friction test device fabricated at the Sandia SUMMIT process. The device produces two-axis motion provided by electrostatic actuation of interdigited comb drives used to pull a beam against a post and rub the two surfaces.

earlier studies on the wear of bulk silicon, using larger scale pin-on-disk testing, suggested mechanisms that are active in metals [11–14], including abrasion, chipping and flattening of protrusions, plasticity and delamination wear.

In this study, on-chip testing and a suite of electron and infrared microscopy techniques were used to investigate wear in micron-scale polycrystalline silicon structural films in ambient air. Examination of wear debris and worn surface regions leads us to propose a mechanism describing wear at the micron-scale.

## 2. Experimental procedures

To study active mechanisms in sliding wear, we have used n-type polysilicon MEMS side-wall friction test specimens with a perflurordecyltrichlorosilane, $CF_3(CF_2)_7(CH_2)_2SiCl_3$, monolayer coating[1] fabricated using the Sandia National Laboratories SUMMIT process (Fig. 1) [15,16]. Specifically, two electrostatic comb-drive actuators create motion in two orthogonal directions. Applying a DC voltage to one of the actuators pulls the beam against a post; sinusoidal AC signals leading to the other, perpendicular, comb drive then cause the beam to rub back and forth against the post (Fig. 1). To determine the normal forces between the beam and the post during the wearing process, the devices were first calibrated. By noting the applied DC voltage in the normal comb drive until it touches the post and using elastic beam bending theory, an estimate of the normal force can be determined as function of the applied voltage to the normal comb drive. More details on the calibration procedure can be found in Ashurst et al. [17]. After running the devices in ambient air (40–50% relative humidity, 22–25 °C) under a normal surface force of ~1 μN at a frequency of 100 to 400 Hz with a sliding amplitude of ~5–15 μm, scanning electron microscopy (SEM) images of worn surfaces and the associated wear debris were used to determine the morphology of the worn areas. The SEM imaging was performed using both a JEOL 6340F Field Emission SEM

(FESEM) and a FEI Dual Beam Focus Ion Beam (DBFIB). Energy dispersive X-ray spectroscopy (EDX) was further utilized to provide qualitative information on the chemical composition of the debris particles and beam surface.

Focused-ion beam (FIB) sample preparation techniques [18] followed by transmission electron microscopy (TEM) observations, utilizing both a 300 kV JEOL 3010 ($LaB_6$ filament) and a 200 kV Philips CM200FEG (field emission gun), were used to acquire more detailed information on the wear debris and worn surfaces. After removing worn beams from the devices and thinning them to electron transparency, worn areas of the beam were observed by TEM and the debris analyzed using both imaging and diffraction modes, the latter giving information regarding the crystal structure. Additionally, analytical TEM, which combines quantitative chemical analysis with high spatial resolution, was used to analyze the chemical composition of the wear debris and worn areas in the beam. In this case, EDX in combination with a reference sample of known composition was used to acquire quantitative information.

Worn beams of the sidewall devices were cut out of the device using the FIB and moved to (half a) copper TEM sample grid (Fig. 2) by means of a sharp tungsten needle, to which the beams were (temporarily) welded using platinum. FIB thinning of these beams was performed after depositing protective layers of platinum on the surface exposed to the ion beam during thinning to electron transparency. First a platinum layer was put down using the electron beam (with minimal surface damage) to protect the sample from damage during deposition of the second, thicker, layer with the ion beam. To thin the beam, slices perpendicular to the worn surface were milled off, starting from the side of the beam that was protected with platinum, i.e., opposite to the side that had been worn. This was necessary to prevent ion implantation during thinning and subsequent damage of the worn surface.

Finally, the devices were run beneath an advanced custom-built infrared (IR) microscope-type system to determine the magnitude of any temperature increases caused by friction in the structures during actuation. The IR system employed liquid nitrogen cooled detectors (InSb based), implemented on a proprietary inspection platform. This system has a spatial resolution of 5 μm and a temperature resolution of 10 mK. Using a semi-quantitative temperature model, an estimate of the local temperature increases was determined.

---

[1] Released via the following steps in solution at room temperature: release etch (buffered HF); rinse with DI water; oxidize with $H_2O_2$; rinse with DI water; transfer to isopropyl alcohol, then *iso*-octane; transfer to 1 mM solution of the monolayer in *iso*-octane; hold in solution for 2 h; transfer to neat *iso*-octane; to isopropyl alcohol; to DI water; remove from DI water and air dry on class 10 clean bench.

## 3. Results and discussion

SEM images of worn silicon beam surfaces and wear debris, shown in Fig. 3, were used to deduce the morphology of the wear particles and worn surfaces. The debris and worn surface morphology appeared similar for devices that were run from hundreds of thousands to several millions of cycles under similar conditions; only the total volume worn increased as the number of cycles increased. The debris particles, which varied in diameter from a minimum of ~50–100 nm to a maximum of ~500 nm (Fig. 3C,D), exhibited a relatively spherical morphology, unlike the more flake-like debris that is often encountered with delamination wear [11]. The worn surface of the beam also showed evidence of long plow tracks (several μm in length), with a width of ~100–400 nm (Fig. 3A,B). This is an order of magnitude larger than the inherent roughness of the sidewalls (~10–15 nm), but is of the same order of magnitude as the wear debris, suggesting that their formation is associated with abrasive wear, caused by third body debris particles.

An approximate chemical composition of the wear debris and the worn surface was determined by EDX in the SEM. As expected, the central region of the beam was found to be pure silicon; however, a higher oxygen content was found in the wear debris, which suggests that the debris is at least partially oxidized silicon (Fig. 4). Indeed, semi-quantitative analysis of these spectra revealed atomic fractions consistent with the debris being $SiO_2$; however, lacking a reference sample with enough area of pure $SiO_2$ to probe with the SEM, the precise chemical composition could not be conclusively determined. The EDX spectra also show a clear carbon peak to the left of the oxygen peak, for both the worn surface and wear debris; additionally, an aluminum peak is visible in the spectrum for the debris particle. The former is an inherent effect of electron microscopy, where carbon gets deposited on the sample surface during imaging; the latter is caused by the aluminum sample holder. No traces of other elements from the coating were found, suggesting that the mono-layer surface coating only delays wear. This is consistent with the fact that for bare silicon devices the debris morphology looks similar, but takes longer to form in large quantities.

Bright-field TEM images and selected-area diffraction (SAD) patterns, shown in Fig. 5, indicate that the debris particles are amorphous. Diffuse rings were found around the forward scattered beam in the diffraction patterns across the particle (Fig. 5B,D). It also appears that the larger debris particles (up to ~500 nm in size) consist of an agglomeration of smaller particles (~50–100 nm). Fig. 5A,C shows different contrast inside the agglomerates, which are bounded by shapes similar to the smaller debris particles. These smaller particles are ~50–100 nm in diameter and do not appear to be made up of even smaller particles, as one might expect from atomic-scale wear of the top silicon dioxide layer and eventually the silicon itself. These observations lead to two conclusions: (i) wear occurs by removal
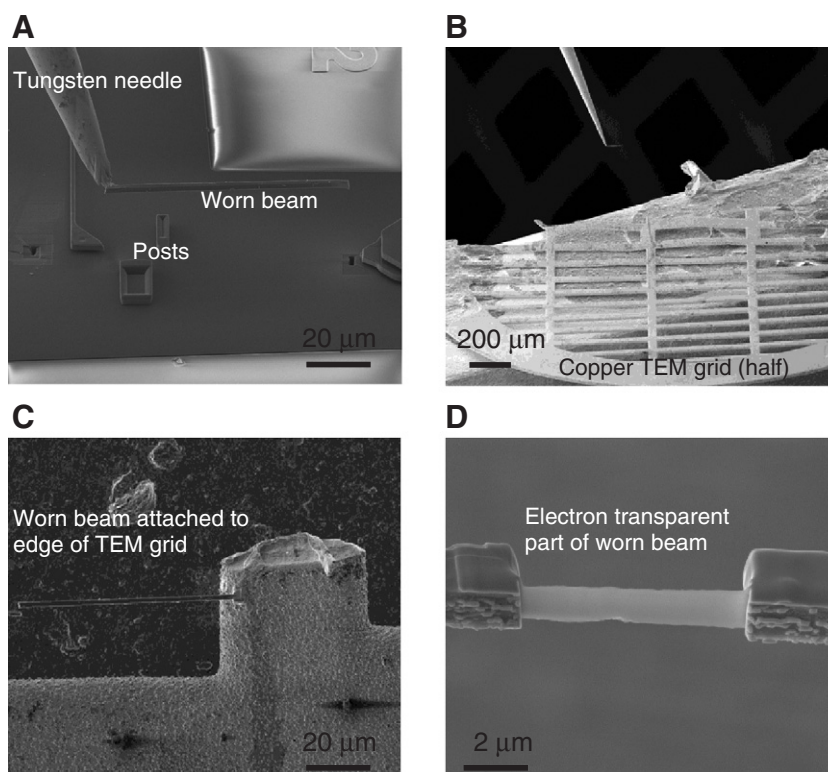


Fig. 2. Focus Ion Beam (FIB) lift-off TEM sample preparation, using Dual Beam FIB mounted with an Omniprobe (tungsten needle in the two top images). (A): Worn beam is cut from device and platinum-welded to the Omniprobe. (B): Sample is moved to half TEM grid (3 mm diameter circular copper grid). (C): Sample attached to TEM grid. (D): Beam thinned to ~100 nm thickness by ion beam in worn region (bottom of sample; edge of thin part); note the protective platinum coating on the facing side that was deposited on the surface before the beam was thinned to protect the sample during thinning. All images are taken using electron imaging at 5 kV.
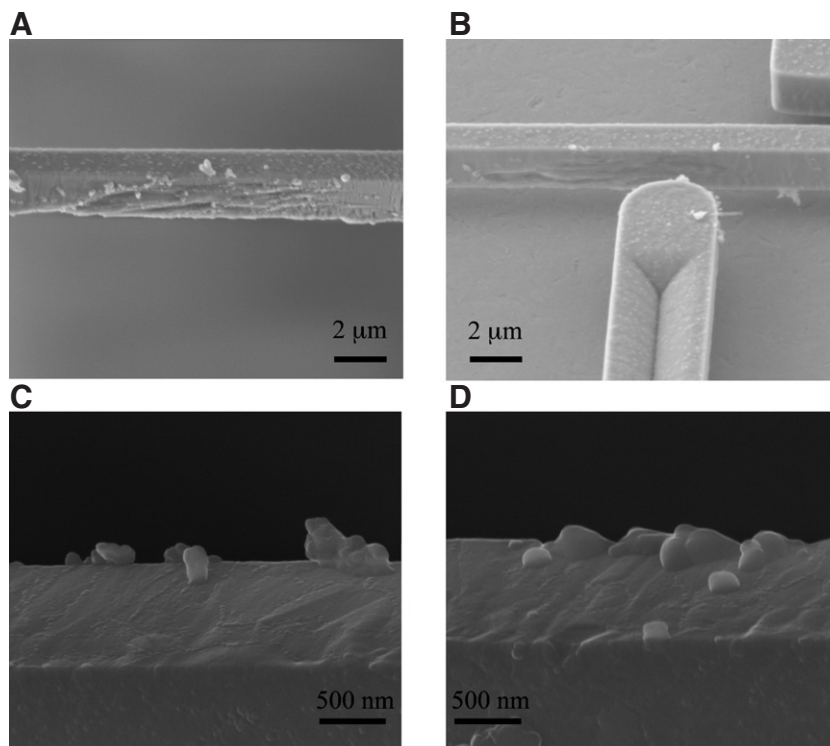
Fig. 3. Typical SEM images of different worn devices after wearing, (A) $\sim 3 \times 10^6$ cycles, (B) $\sim 5 \times 10^5$ cycles; (C), (D) wear debris ($\sim 100$–$500$ nm in size) on the surface of a worn beam after lift-off from the chip. In (C) and (D) the worn surface is on a face of the beam that is not directly visible; debris particles, however, are clearly visible. (A), (B) are taken at 5 kV and (C), (D) at 18 kV.

of 50–100 nm particles and does not occur by atomic-scale grinding, and (ii) because the inherent grain size of the polysilicon in the beam is $\sim 500$ nm (Fig. 7), this wear debris must be generated by adhesion and fracture through the grain. The latter happens when the work of adhesion between the two surfaces is higher than the energy needed for crack propagation within a silicon grain.

TEM EDX analysis confirmed that the oxygen content of the debris particles was higher than inside the beam (Fig. 6). Quantification of these EDX results using a reference $SiO_2$ sample revealed a silicon–oxygen atomic ratio of $\sim 50:50$ in the middle of the particles but $\sim 34:66$ at the edges. This suggests that although the debris particles are amorphous, only the edge is stoichiometric $SiO_2$ and the entire particle does not consist of



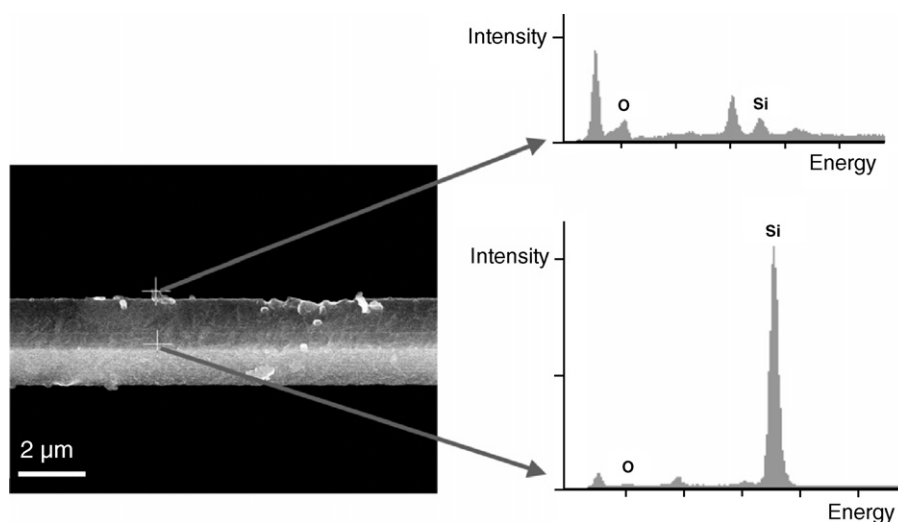Fig. 4. SEM EDX of the worn surface of the silicon beam at $\sim 30°$ tilt, (bottom right) and of wear debris (top right). The debris particles appear to be $SiO_2$, although no reference sample was used to calibrate these quantitative values. Substantial C and Al peaks are visible in the spectrum of the debris; however, the Al is from the sample holder and the C is a typical artifact caused by beam-induced contamination.
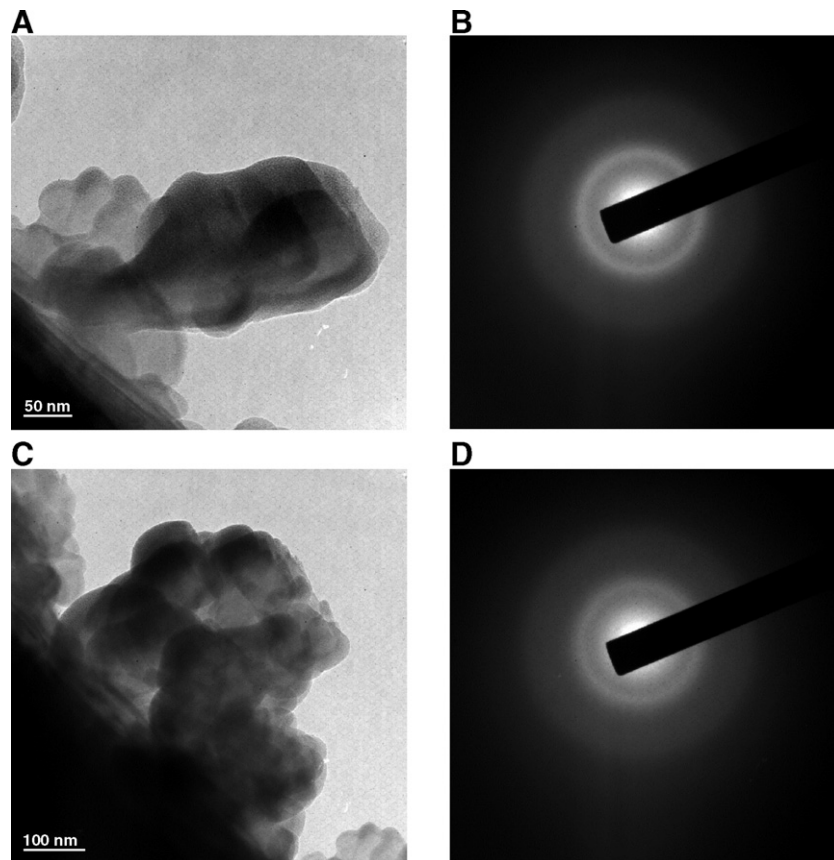
Fig. 5. Typical TEM bright-field images (A), (C) and accompanying diffraction patterns (B), (D) of debris particle agglomerates, show the particles to be amorphous. The dark areas in the bottom left of both images are the surface of the worn beam.

$SiO_2$ (for which a 33 : 66 ratio would be expected for the entire particle). Accordingly, we can conclude that the particles oxidize heavily when they are worn off and are comprised of an amorphous $SiO_2$ shell on an amorphous Si core. It is not possible at this stage to define with complete certainty when the particles become amorphous or what causes this to happen, although it most likely occurs after they are removed from the grain and could be aided by high local contact stresses (which can be expected to be as large as several GPa [19]).

It was also apparent that sections of the worn beam exhibited a surface layer with a microstructure that was quite distinct from the rest of the beam, as shown in the TEM bright-field image in Fig. 7 (left panel). (Here the top edge is the surface where the beam has been worn and where a section of this surface layer is shown; at the bottom edge, the remainder of the protective Pt layer can be seen). These surface layers varied in their in-plane thickness from ~20 nm to almost 200 nm, and appeared to be amorphous, whereas the beam itself is populated with ~500 nm sized polycrystalline silicon grains. Closer investigation revealed that this surface layer is actually nano-crystalline, as typified by the region in Fig. 7(right panel) where the layer is thicker (~200 nm). Because of the sharp rings visible in the diffraction pattern, it can be concluded that there are numerous small crystals present in this relatively small volume. These nano-crystals are much smaller than the overall grain size and are even smaller than the debris particles. Control samples of areas that were not

subject to wear confirmed that the microstructure inside the beam looked similar in both cases. However, these control samples showed no evidence of a surface layer with a different microstructure, as was observed in worn areas.

EDX measurements revealed that the oxygen content was higher inside this surface layer than in the rest of the beam (Fig. 8). Quantitative analysis of the EDX results with respect to a $SiO_2$ reference sample shows that the layer is not fully $SiO_2$ (Si : O = 65 : 35 at.% in the marked area; in other areas of the layer Si : O atomic percent ratios of 80 : 20 have been recorded). This is consistent with the fact that the layer is actually nano-crystalline, with Si as the dominant species, although with a significant degree of oxidation. These results suggest that smaller (≪100 nm) partly oxidized debris particles, created during actuation, become attached to the beam and lead to the formation of this surface layer. These particles could be originating from the initial surface asperities, which were ~10–15 nm in size.

Finally, infrared (IR) microscopy images were obtained during device operation to gather information on the possible local temperature increases at wearing surface. Fig. 9 shows an increase in contrast, representing temperature changes in the beam that is being worn, as well as in the comb drives. Based on temperature models used with similar experiments with this IR microscope system [7], the increase in the temperature experienced by the MEMS parts at the point of contact is
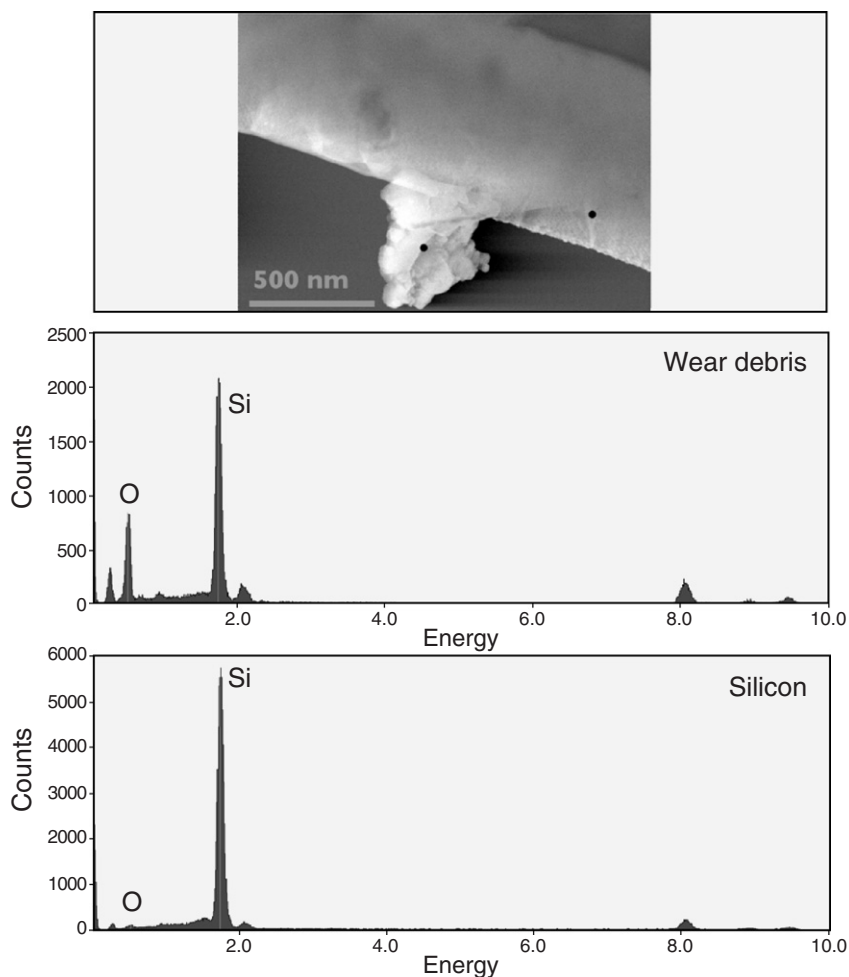
Fig. 6. TEM EDX of wear debris and beam. The dots in the image, which show the beam and a large debris agglomerate on the surface, indicate where the two X-ray spectra were acquired. The beam consists of silicon, whereas the debris particle has a much higher oxygen concentration.

estimated to be no higher than several K, consistent with rough estimates calculated using simplistic flash temperature models [20]. Similar temperature rises are seen at the comb drive, presumably because of frictional energy caused by viscous damping in the narrow gaps of the quickly moving comb drive. Such variations in temperature are unlikely to promote extensive
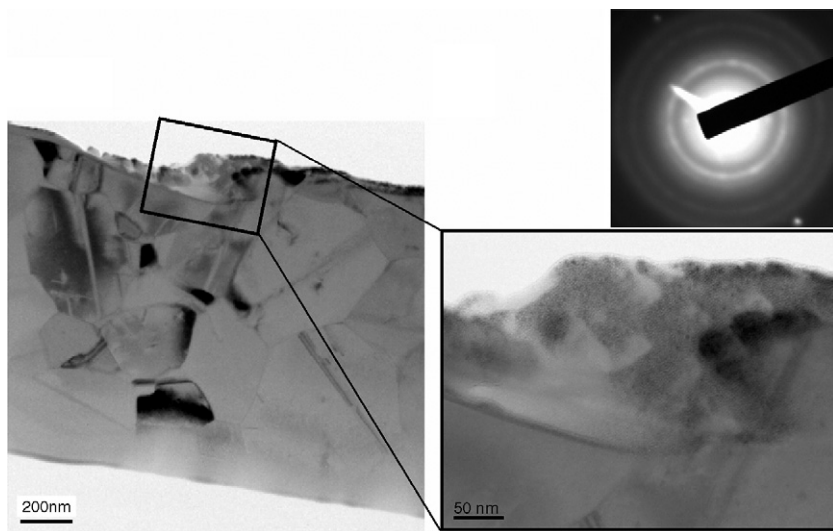


Fig. 7. TEM bright-field image and selected area diffraction (SADIFF — upper right) of surface layer in worn area of beam. The image shows that the top surface layer, which has been worn, has a different microstructure than the beam. SADIFF shows the surface layer is nano-crystalline.
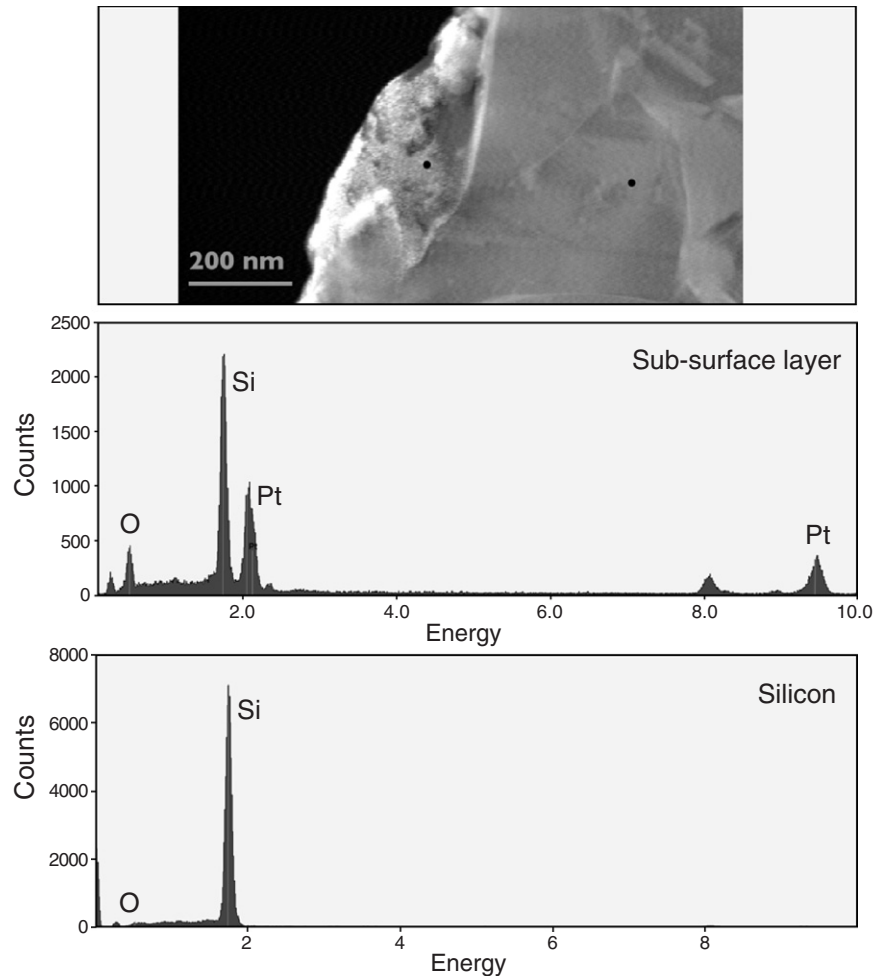
Fig. 8. TEM EDX of surface layer. The dots in the image, which show part of the worn surface layer and the microstructure of the silicon beam, indicate where the X-ray spectra were acquired. The beam consists of silicon, whereas the surface layer has a higher oxygen concentration. Note: the platinum peak is an artifact of the FIB sample preparation method, and represents ~5 at.% of the surface composition.

dislocation plasticity, which is generally observed above ~500 °C [21]. It is feasible that more significant temperature increases are generated at very localized regions, e.g., less than 1 μm, such as the frictional contact area and asperity/asperity or debris particle/surface interaction areas; however, such localized regions are beyond the spatial resolution limit (~5 μm) of most, if not all, IR microscope systems. Additionally, the TEM images of FIB cross-sectioned samples did not reveal any evidence of additional dislocation pile-ups below or in the surface layer after wearing (Fig. 7). This strongly suggests that dislocation plasticity is indeed not an active mechanism during wear at these size-scales.
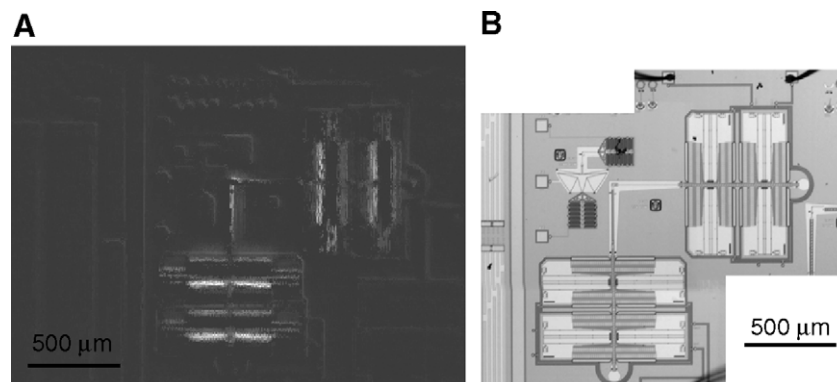


Fig. 9. IR microscopy image of operating wear device (A): ambient air, 3 min at 200 Hz. The image shows a small temperature increase in the silicon beam and comb drive. For comparison, an optical micrograph of the same device is given (B).

## 4. Conclusions

On-chip polycrystalline silicon side-wall friction test specimens have been used to study active mechanisms in the sliding wear of polysilicon at micron-scale dimensions in ambient air. Wear debris and wearing surfaces were examined using electron and infrared microscopy. Observations show an initial regime of adhesive wear, where debris particles, ~50–100 nm in size, are created by surface adhesion and fracture through the silicon grains. These particles subsequently oxidize and agglomerate into large (up to ~500 nm) debris clusters. This wear debris is amorphous (with an amorphous silicon core and a silica outer layer) and initiates a second wear regime where abrasion dominates. Plowing tracks are created on the worn surface by these debris particles and clusters, caused by cracking rather than plastic deformation. The exact driving force for the amorphization of the silicon debris is unknown and will be the focus of future studies, but it is likely caused by high local contact stresses. Concomitantly, a nano-crystalline surface layer (thickness ~20–200 nm), with higher oxygen content than the rest of the beam (up to 35 at.%), forms during wear by partial oxidation of nano-crystalline silicon particles and the worn surface. These nano-crystals, which are smaller than debris particles found around the worn surface, are enclosed in this layer. Finally, IR microscopy revealed no evidence of significant temperature increases, nor did TEM show any dislocation pile-ups, ruling out any mechanisms that include (high-temperature) dislocation plasticity.

## Acknowledgements

## References

[1] A.D. Romig Jr., M.T. Dugger, P.J. McWhorter, Acta. Mater. 51 (2003) 5837.
[2] R. Maboudian, W.R. Ashurst, C. Carraro, Tribol. Lett. 12 (2002) 95.
[3] D.M. Tanner, W.M. Miller, W.P. Eaton, L.W. Irwin, K.A. Peterson, M.T. Dugger, D.C. Senft, N.F. Smith, P. Tangyunyong, S.L. Miller, IEEE International Reliability Physics Symposium Proceedings, 1998.
[4] D.M. Tanner, J.A. Walraven, L.W. Irwin, M.T. Dugger, N.F. Smith, W.P. Eaton, W.M. Miller, S.L. Miller, IEEE International Reliability Physics Symposium, San Diego, U.S.A., 1999.
[5] S.T. Patton, W.D. Cowan, K.C. Eapen, J.S. Zabinski, Tribol. Lett. 9 (2000) 199.
[6] S.T. Patton, J.S. Zabinski, Tribol. Int. 15 (2002) 373.
[7] C.L. Muhlstein, E.A. Stach, R.O. Ritchie, Acta. Mater. 50 (2002) 3579.
[8] D.H. Alsem, E.A. Stach, C.L. Muhlstein, R.O. Ritchie, Appl. Phys. Lett. 86 (2005) 1914.
[9] C.L. Muhlstein, S.B. Brown (Eds.), Mechanical Properties of Structural Films, ASTM STP, vol. 1413, American Society for Testing and Materials, West Conshohocken, PA, 2001, p. 333.
[10] S. Brown, J. Gilbert, H. Guckel, R. Howe, G. Johnson, P. Krulevitch, C. Muhlstein (Eds.), Microelectromechanical Structures for Materials Research, vol. 518, Materials Research Society, San Francisco, CA, 1998.
[11] R.G. Bayer, Wear 69 (1981) 235.
[12] S. Danyluk, R. Reaves, Wear 77 (1982) 81.
[13] S. Danyluk, J.L. Clark, Wear 103 (1985) 149.
[14] D.E. Kim, N.P. Suh, Wear 149 (1991) 199.
[15] More information on the SUMMIT process at: http://mems.sandia.gov.
[16] D.C. Senft, M.T. Dugger, SPIE 1997, 3224 (1997) 31.
[17] W.R. Ashurst, C. Yau, C. Carraro, R. Maboudian, M.T. Dugger, J. Microelectrom. Syst. 10 (2001) 41.
[18] L.A. Giannuzzi, F.A. Stevie (Eds.), Introduction to Focused Ion Beams: Instrumentation, Theory, Techniques and Practice, Springer, New York, 2004.
[19] K.L. Johnson, Contact Mechanics, Cambridge University Press, Cambridge UK, 1985.
[20] J.F. Archard, Wear 2 (1959) 438.
[21] K. Sumino, Metall. Mater. Trans., A 30A (1999) 1465.